

# Adaptive Optics: An Introduction

Claire E. Max

University of California Observatories  
Department of Astronomy and Astrophysics  
University of California  
1156 High Street  
Santa Cruz, CA 95064 USA  
<mailto:max@ucolick.org>

## OVERVIEW OF ADAPTIVE OPTICS FOR ASTRONOMY

Adaptive optics is a technology that corrects for distortions in optical systems. In the context of ground-based astronomy, adaptive optics is used to compensate for rapidly changing image distortions due to turbulence in the Earth's atmosphere. At the core of an adaptive optics system is a deformable mirror: a mirror that can change its shape hundreds or thousands of times a second, in order to cancel out the aberrations due to atmospheric turbulence in real time. Because the primary mirrors of ground-based telescopes are typically heavy and cannot be moved quickly (even segmented mirrors are massive), the deformable mirror is a separate unit placed after the light has already been reflected from the primary mirror. A variety of technologies are used today for deformable mirrors, ranging from adaptive secondary mirrors up to a meter in diameter to tiny MEMS<sup>\*</sup> mirrors less than a cm in size. One or more wavefront sensors rapidly measure the distorted wavefront of the light incident on the telescope. To date most astronomical wavefront sensors have been Shack-Hartmann sensors or curvature sensors; pyramid wavefront sensors show great promise for high-performance adaptive optics. After the wavefront sensor has measured the incident optical distortions, a real-time control system calculates the corrective signal to be sent to the actuators of the deformable mirror, in order to correct the wavefront. The process then repeats. Because the wavefront is measured hundreds or thousands of times a second, a relatively bright point-like reference source is needed in order for these measurements to have an acceptable signal to noise ratio. This reference source must be close to the astronomical object being imaged, so that the light from the reference source and from the astronomical target both pass through the same turbulence. The reference source can be a star, usually with magnitude  $R \leq 14-15$ , or an "artificial beacon" made by a laser beam that is projected upwards into the atmosphere. Today's laser guide stars use either Rayleigh scattering from air molecules at an altitude up to 15 km, or resonant scattering from sodium atoms at an altitude of 95 km, in order to make the "artificial beacon" needed to measure atmospheric turbulence. The latest astronomical adaptive optics systems employ multiple laser beacons to measure the turbulence over a wider field of view using tomographic methods, and correct for atmospheric distortions using methods such as Multi-Conjugate Adaptive Optics, Ground-Layer Adaptive Optics, and Multi-Object Adaptive Optics.

---

\* Micro-Electro-Mechanical Systems. These devices are produced using methods similar to those used to manufacture computer chips.

## TABLE OF CONTENTS

I.	Brief overview of adaptive optics.....	4
	A. Telescope performance, ideal and real .....	4
	B. Nature and origins of atmospheric turbulence .....	6
	C. A quantitative description of atmospheric turbulence .....	7
	D. How adaptive optics improves image quality .....	8
II.	The effect of turbulence strength on adaptive optics design and performance .....	9
	A. The atmospheric coherence length $r_0$ .....	9
	B. Impact of $r_0$ on adaptive optics systems: number of actuators .....	10
	C. Impact of $r_0$ on adaptive optics systems: temporal response .....	11
	D. Impact of $r_0$ on adaptive optics systems: isoplanatic angle.....	12
III.	Bibliography .....	14

## [KEYWORDS]

adaptive optics, atmospheric turbulence, deformable mirrors, wavefront sensors, real-time control, adaptive secondary, MEMS, membrane mirror, Shack-Hartmann sensor, curvature sensor, pyramid sensor, laser guide star, artificial beacon, Rayleigh guide star, sodium guide star, Strehl ratio, wavefront error, error budget, diffraction limit, lenslet, atmospheric turbulence, actuator, optical aberration

## [LIST OF ABBREVIATIONS]

AO - adaptive optics

DM - deformable mirror

WFS - wavefront sensor

LGS - laser guide star

TT - tip-tilt

FWHM - full width at half maximum

$r_0$  - atmospheric coherence length or Fried parameter

HST - Hubble Space Telescope

IR - infrared

PSF - point spread function

arc sec - one arc second of angular diameter

## I. BRIEF OVERVIEW OF ADAPTIVE OPTICS

Adaptive optics is a technology that removes aberrations from optical systems, through use of one or more deformable mirrors which change their shape to compensate for the aberrations. In the case of adaptive optics (hereafter AO) for ground-based telescopes, the main application is to remove image blurring due to turbulence in the Earth's atmosphere, so that telescopes on the ground can "see" as clearly as if they were in space. Of course space telescopes have the great advantage that they can obtain images and spectra at wavelengths that are not transmitted by the atmosphere. This has been exploited to great effect in ultra-violet bands, at near-infrared wavelengths that are not in the atmospheric "windows" at J, H, and K bands, and for the mid- and far-infrared. However since it is much more difficult and expensive to launch the *largest* telescopes into space instead of building them on the ground, a very fruitful synergy has emerged in which images and low-resolution spectra obtained with space telescopes such as HST are followed up by adaptive-optics-equipped ground-based telescopes with larger collecting area.

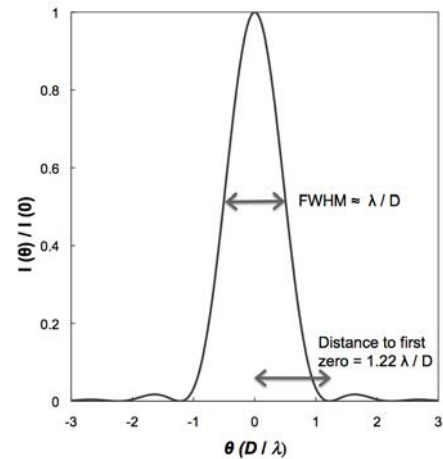
Astronomy is by no means the only application for adaptive optics. Beginning in the late 1990's, AO has been applied with great success to imaging the living human retina (Porter 2006). Many of the most powerful lasers are using AO to correct for thermal distortions in their optics. Recently AO has been applied to biological microscopy and deep-tissue imaging (Kubby 2012). This Chapter will focus on the applications of adaptive optics for improving the spatial resolution of ground-based astronomical telescopes.

There are a series of excellent reviews on this topic, to which the reader is referred for information about the history of the field. These include two articles in Annual Reviews of Astronomy and Astrophysics (Beckers 1993, Davies and Kasper 2012), and a review by Roggeman, Welsh, and Fugate in Reviews of Modern Physics (1997). For the early history of adaptive optics and laser guide stars, the Lincoln Laboratory Journal (1992) contains excellent discussions of adaptive optics and laser guide star programs developed by and for the US military. A monograph by Dutton (2009) details AO development specifically in the US Air Force. The textbooks by Hardy (1998), Roddier (1999), and Tyson (2012) also have good information about historical adaptive optics systems for ground-based telescopes.

### A. TELESCOPE PERFORMANCE, IDEAL AND REAL

In principle, telescopes seeking the highest possible spatial resolution should be able to form images at their diffraction limit. For example for a point source viewed through a diffraction-limited circular telescope aperture, the angular distance from the center of the image to the first zero of its diffraction pattern would be  $\vartheta_{dl} = 1.22(\lambda / D)$ , where  $\lambda$  is the wavelength at which the observation is being obtained and  $D$  is the telescope diameter. This is also the minimum angular separation between two point sources at which an observer can distinguish that there are two separate images (Rayleigh's criterion). The full width at half maximum of a single diffraction-limited source viewed through a circular aperture is  $\vartheta_{FWHM} \approx (\lambda / D)$ . These relations are shown in Figure 1.

Figure 1 - Intensity distribution of a point source that has been imaged through a circular aperture of diameter  $D$ , at a wavelength  $\lambda$ . The distance from the axis to the first zero of the diffraction pattern is  $1.22 \lambda/D$ ; the full width at half maximum of the central core is  $\sim \lambda/D$ .



The optics for the highest-resolution space telescopes (such as the Hubble Space Telescope) are polished to exacting tolerances that will allow them to achieve this ideal diffraction limit. However for ground-based telescopes, it is turbulence in the Earth's atmosphere rather than the quality of their optics that limits the achievable spatial resolution. Not only does atmospheric turbulence make stars twinkle; it also blurs the image of a point source (such as a distant star) far beyond the ideal diffraction-limited size  $\vartheta_{FWHM} \approx (\lambda/D)$ . This causes drastic degradation in image quality. At good astronomical telescope sites, real stellar images are about 1 arc sec in diameter and have no diffraction-limited core like the one shown in Figure 1. By contrast the ideal diffraction-limited diameter  $\vartheta_{FWHM}$  for an 10-meter telescope observing at a wavelength  $\lambda = 1 \mu\text{m}$  is about 0.02 arc sec, which is 50 times smaller than the typical "seeing-limited" diameter (1 arc sec) of a point source seen through atmospheric turbulence. Thus if one can fully correct for the blurring effects of turbulence in the Earth's atmosphere, huge gains in spatial resolution are possible. This is illustrated using a modest 1-m telescope in Figure 2.

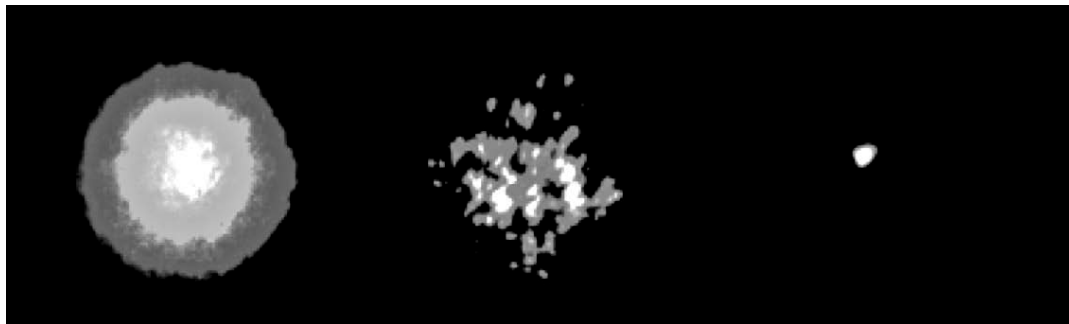


Figure 2 Three images of the bright star Arcturus, obtained with the 1-m diameter Nickel telescope at Lick Observatory. Left: Uncorrected or "seeing limited" image, approximately 1 arc sec in diameter. Middle: A very short exposure image of Arcturus. This snapshot had a sufficiently short integration time that the turbulence did not change during the exposure. The structure is dominated by many small "speckles," each at about the diffraction limit of the telescope. The spatial envelope of the speckles is still of order 1 arc sec. Right: Adaptive optics-corrected image of Arcturus. The core of the image is approximately the size of the diffraction limit. The shape is a bit distorted, in this case due to uncorrected static aberrations in the optics and the telescope.

The degree of correction of an adaptive optics system is frequently quantified by the "Strehl ratio", which is the peak on-axis intensity of the actual image of a point source, divided by the peak intensity which that same source would have if the telescope were diffraction-limited. The Strehl of typical seeing-limited ground-based telescopes is at most a few percent, and usually less. Today (as

of 2012) the record Strehl for an 8-10 meter class ground-based telescope using adaptive optics is held by the Large Binocular Telescope: greater than 80% Strehl at a wavelength of  $1.6 \mu m$ , using a bright reference star (Esposito et al. 2011). Between 2000 and 2010, bright-natural-star Strehl ratios for on-axis imaging at K band ( $\lambda = 2.2 \mu m$ ) on the various 8-10 meter telescope AO systems were between 35 - 60% on nights of good seeing ( $r_0 > 15 \text{ cm}$  at K band).

## B. NATURE AND ORIGINS OF ATMOSPHERIC TURBULENCE

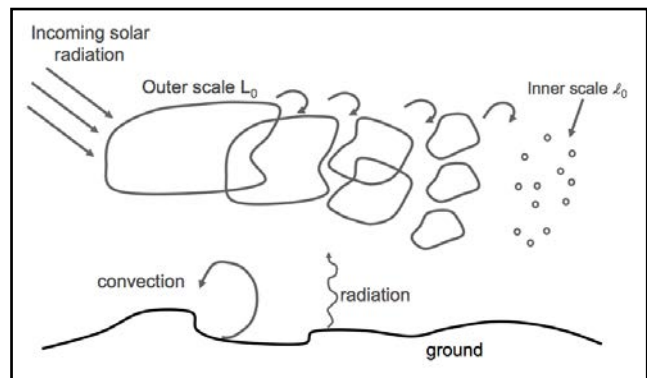
Turbulence in the Earth's atmosphere is caused by many physical phenomena. The atmospheric boundary layer is the part of the atmosphere closest to the ground, whose state and wind speeds are influenced directly by the presence of the Earth's surface. The boundary layer is almost continuously turbulent throughout its volume, and its thickness varies from a few hundred meters at night to as much as a few km during the day when solar heating of the Earth's surface is strong. The result is that solar astronomers have to work with a thick and messy boundary layer, whereas at night both the thickness and turbulence strength decrease. Above the boundary layer is the so-called "free atmosphere" in which turbulence is strong in frequently-discrete layers of relatively large, but not infinite, horizontal size. Turbulence in the free atmosphere has a local maximum at the tropopause (height 10-15 km), which is where the atmospheric temperature stops increasing with altitude, and begins to decrease again in the lower stratosphere. The tropopause is the site of large amounts of wind shear, which causes shear-flow instabilities.

In addition to these naturally caused sources of turbulence, astronomers have, in the past, made even more turbulence within their own telescope domes by local heat sources such as uncooled electronics or a warm telescope mirror which cause convection within the dome itself. These effects, which collectively cause "dome seeing," have increasingly been mitigated through use of external cooling and by removing significant heat sources from the dome entirely.

The spectrum of turbulence in the atmosphere (that is, the turbulence strength at different spatial scales) is frequently well-described by the predictions of Kolmogorov turbulence (e.g. Tatarski, 1961), in which the three-dimensional power spectral density for velocity fluctuations is  $\Phi(\vec{k}) \propto k^{-11/3}$ , where  $k = 2\pi / \lambda$  is the wavenumber corresponding to fluctuations of scale  $\lambda$ . This spectrum can be derived by dimensional analysis using the following assumptions:

1. Energy is added to the system at the largest scale - the "outer scale"  $L_0$
2. Then energy cascades from larger to smaller scales. The size range over which this takes place is called the "Inertial range".
3. Finally, the eddy size becomes so small that it is subject to dissipation from viscosity at the so-called "Inner scale"  $\ell_0$

Figure 3 Schematic showing the energy flow in Kolmogorov turbulence. Incoming solar radiation provides the energy input at the largest spatial scale  $L_0$ , called the outer scale. Energy then flows from larger eddies to smaller ones, and is finally dissipated due to viscosity at the "inner scale"  $\ell_0$ .



The scenario is illustrated schematically in Figure 3. In the Earth's atmosphere,  $L_0$  ranges from 10's to 100's of meters;  $\ell_0$  can be as small as a few mm

### C. A QUANTITATIVE DESCRIPTION OF ATMOSPHERIC TURBULENCE

For optical and infrared astronomers the main deleterious effect of atmospheric turbulence is to cause fluctuations in the local index of refraction. The index of refraction  $n$  of air is very close to unity, so it is usually written in terms of its deviation from unity:

$$N \equiv (n-1) \times 10^6 = 77.6 \left( 1 + \frac{7.52 \times 10^{-3}}{\lambda^2} \right) \times \left( \frac{P}{T} \right) \quad (1)$$

where  $n$  is the index of refraction,  $N$  is  $10^6$  times its difference from unity,  $P$  is the atmospheric pressure in millibars,  $T$  is the temperature in K, and  $\lambda$  is the observing wavelength in microns. Since turbulent motions in the Earth's atmosphere are very subsonic, pressure differences are rapidly smoothed out by the propagation of sound waves. Hence the only atmospheric quantity whose variability affects the index of refraction  $n$  is a change in the temperature  $\delta T$ . Note the very weak dependence of the index of refraction on observing wavelength, valid for visible and near-infrared light. At these wavelengths the index of refraction of air is achromatic to a very good approximation. From Equation (1), the index of refraction  $n$  varies with temperature as

$$\delta N \cong -77.6 \times (P/T^2) \delta T \quad (2)$$

The effect of fluctuations in the index of refraction is to cause many small deviations in the direction of propagation of starlight as it travels downward through the atmosphere and traverses many regions with slightly difference indices of refractions. Cumulatively these many small-angle deflections of the incoming rays add up, and can lead to wavefronts that are significantly distorted, as shown in Figure 4.

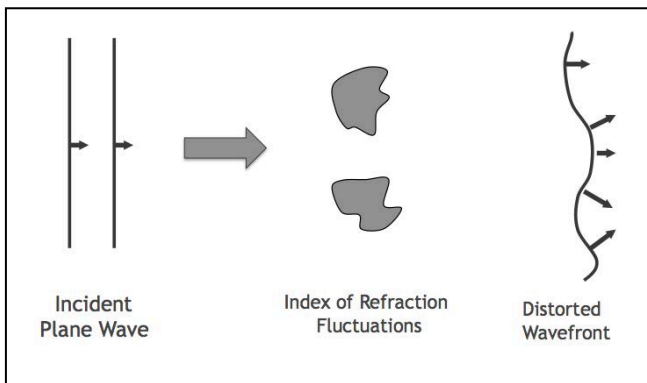


Figure 4 A plane wave incident at the top of the atmosphere is refracted by small amounts as it passes through many regions with different indices of refraction. By the time it reaches a telescope at the bottom of the atmosphere, the wavefront is significantly aberrated. Adaptive optics can restore the wavefront almost to its original flat shape.

The physically important quantity for describing the effect of index of refraction fluctuations  $\delta N$  on image formation is the "structure function"  $D_N(r)$ , which describes the mean square difference between the index of refraction  $N$  at two spatial locations that are separated by a distance  $r$ . One can show (Hardy, 1998, Roddier 1999, and references therein) that if the atmospheric turbulence has a Kolmogorov spectrum, the structure function for index of refraction fluctuations is proportional to the distance between the two points to the 2/3 power:

$$D_N(r) \equiv \left\langle [N(\vec{x}) - N(\vec{x} + \vec{r})]^2 \right\rangle \propto r^{2/3} \quad \text{or} \quad D_N(r) = C_N^2 r^{2/3} \quad (3)$$

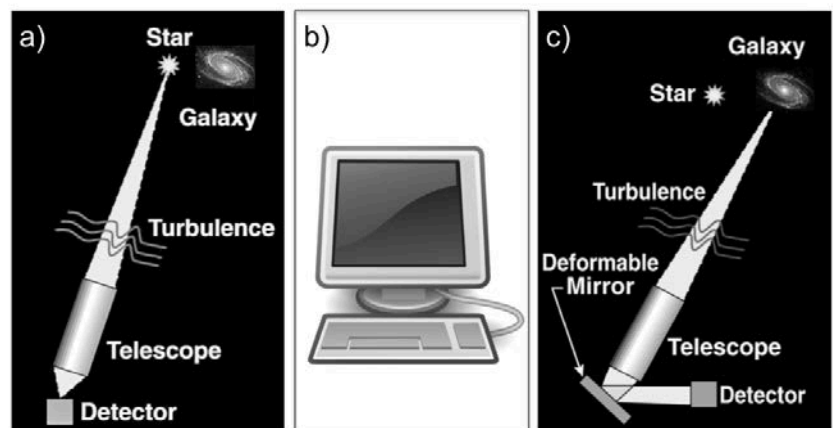
The quantity  $C_N^2$  is introduced as the proportionality factor between  $D_N(r)$  and  $r^{2/3}$ . Its value parameterizes the strength of the turbulence. When turbulence is stronger (larger  $C_N^2$ ), the mean square difference in the index of refraction at two points separated by a fixed distance  $r$  will increase. Similarly, for a fixed turbulence strength, the mean square difference in index of refraction will increase as the separation between two points increases.

In the atmosphere, of course, the strength of the turbulence varies with altitude  $z$ . This is usually taken into account by letting the proportionality factor vary with altitude, so that  $D_N(r, z) = C_N^2(z)r^{2/3}$ . This *ansatz* thus allows us to achieve a separation of variables in describing the optical effects of atmospheric turbulence. Section II will exploit this relation quantitatively: in practice, the separation of variables will mean that many quantities that determine the requirements of AO systems depend on the integrated value of  $C_N^2(z)$  with respect to altitude  $z$ . This greatly simplifies the design of AO systems, because fine details of the vertical profile of  $C_N^2$  are then not important.

#### D. HOW ADAPTIVE OPTICS IMPROVES IMAGE QUALITY

Adaptive optics systems correct for turbulence-induced optical aberrations in three steps. In the simplest form, these are: a) Using a reference source (e.g. a bright star) close to the astronomical object of interest to measure the distorted wavefront after it has been reflected from the telescope's primary mirror. A fast detector must be used, because the distorted wavefront is always changing as the wind advects turbulent eddies across the telescope pupil. b) Calculating on a computer the signals that must be sent to a special deformable mirror placed after the primary mirror of the telescope, in order to correct the aberrated wavefront. c) Applying this computed correction to the deformable mirror, so that the light from both the reference star and the astronomical object of interest bounce off the deformable mirror and are corrected. Since the measurement process and the computation both take time, and since the turbulence above the telescope is changing in the meantime, this process must be repeated over and over again in order to "keep up" with the evolving pattern of turbulence. The progression is shown schematically in Figure 5.

Figure 5 Schematic showing three steps in the operation of a simple closed-loop adaptive optics system. a) If one wants to obtain a clear image of an astronomical source such as a galaxy, one finds a bright star that is close enough to the galaxy that the light from both the star and the galaxy pass through the same turbulence. A fast detector is used to measure the shape of the turbulent wavefront from the star. b) From these data, a fast computer calculates the voltage signals that must be sent to the deformable mirror in order to correct the turbulence-induced aberrations. c) Light from both the reference star and the galaxy are reflected off the deformable mirror, so that aberrations are removed from both.



Adaptive optics corrections are not perfect. Inevitably some aberrated light remains in the image. For an image of a point-source such as a star, light from this uncorrected atmospheric aberration remains in a "halo" with the same extent as the original seeing-disk, usually of order an arc second. In addition the adaptive-optics-corrected core, of angular extent  $\lambda / D$ , can show residual distortions due to uncorrected optical aberrations in the instrument or telescope optics, as shown in the right panel of Figure 2.

## II. THE EFFECT OF TURBULENCE STRENGTH ON ADAPTIVE OPTICS DESIGN AND PERFORMANCE

### A. THE ATMOSPHERIC COHERENCE LENGTH $r_0$

Qualitatively, a key issue for the design of adaptive optics systems is: what is the distance on the primary mirror over which the phase of the incident wavefront becomes decorrelated? One can intuit from Equation (3) that the "coherence length" of index of refraction fluctuations will get shorter as the turbulence strength increases: for a constant value of  $D_N$  and an increasing value of  $C_N^2$ ,  $r$  must decrease. A convenient way to quantify this is by defining an "atmospheric coherence length"  $r_0$  which is a function of  $C_N^2$ , and then expressing the impact of atmospheric turbulence on image formation and AO correction as a function of  $r_0$ .

There are several equivalent ways to define  $r_0$ , the atmospheric coherence length, also referred to as the "Fried Parameter" after David Fried who first introduced it (Fried, 1965). The most useful of these are:

1.  $r_0$  is that telescope diameter where the optical transfer functions of the telescope and the atmosphere are equal.
2.  $r_0$  is the separation between two points on the telescope's primary mirror where the wavefront's phase correlation has fallen by  $1/e$ .

The quantity  $(D/r_0)^2$  is also the approximate number of speckles in a short-exposure image of a point source (see Figure 2). The above definitions mean that if you are working with a telescope with diameter  $D < r_0$ , there will be no benefit to using adaptive optics because the phase will already be coherent over the whole telescope aperture. For telescopes with diameter  $1 \leq D \leq$  a few times  $r_0$ , the dominant effect of atmospheric turbulence is to cause image wander; if this is corrected via a tip-tilt system, there is no need for higher-order adaptive optics. As the quantity  $(D/r_0)$  becomes considerably larger than unity, the complexity of the AO system required to correct images becomes higher and higher.

Quantitatively,  $r_0$  depends on the strength of atmospheric turbulence  $C_N^2(z)$ , on the wavelength at which the image is being observed  $\lambda = 2\pi/k$ , and on the zenith angle  $\zeta$ :

$$r_0 = \left[ 0.423k^2 \sec \zeta \int_0^\infty C_N^2(z) dz \right]^{-3/5} \propto \lambda^{6/5} (\sec \zeta)^{-3/5} \left[ \int_0^\infty C_N^2(z) dz \right]^{-3/5} \quad (4)$$

The coherence length  $r_0$  is smaller when turbulence is strong ( $C_N^2$  is large), as we inferred from Equation (3). In addition  $r_0$  is larger at longer wavelengths  $\lambda$ ; this is because a given deformation in the wavefront, measured for example in  $\mu\text{m}$  of peak-to-valley wavefront distortion, becomes a smaller and smaller fraction of a wavelength as the wavelength becomes longer. Finally,  $r_0$  quickly becomes smaller as the telescope points closer to the horizon (larger zenith angles  $\zeta$ ), because the path length over which the turbulence integral is being integrated is significantly longer at large zenith angles.

Usually the value of  $r_0$  is stated at  $\lambda = 0.5\mu m$  wavelength for reference purposes, and at zenith angle  $\zeta = 0$ . It is then up to the AO user or designer to scale  $r_0(\lambda = 0.5\mu m)$  by  $\lambda^{6/5}$  and by  $(\sec\zeta)^{-3/5}$  in order to assess the effects of turbulence at your observing wavelength and zenith angle. At excellent sites such as Mauna Kea in Hawaii, with an altitude of 14,000 feet,  $r_0(\lambda = 0.5\mu m) \cong 10 - 30\text{ cm}$ . At lower continental observatory sites in North America, typical values of  $r_0$  might be as low as a few cm on a very turbulent night, and up to 10 - 20 cm on good nights. In all cases  $r_0$  is highly variable from night to night, and can vary quite a bit within a night.

### B. IMPACT OF $r_0$ ON ADAPTIVE OPTICS SYSTEMS: NUMBER OF ACTUATORS

A useful way to view adaptive optics system design is to think of dividing the primary mirror into "sub-apertures" of diameter  $d \sim r_0$ . The primary mirror is re-imaged onto the much-smaller deformable mirror via a pupil relay, so that the deformable mirror is a minified version of the telescope's primary mirror. Hence there will be the same number of subapertures on the deformable mirror as on the primary. Since the wavefront phase is reasonably coherent across a distance  $r_0$ , one can choose the number of actuators on the deformable mirror in such a way that the re-imaged value of  $r_0$  corresponds to the inter-actuator spacing of the deformable mirror. In this case, the phase of the wavefront remains coherent within one subaperture, so that a well-defined correction can be applied, as sketched in Figure 6. Then based on the ratio of the area of the primary mirror to the area of one sub-aperture, the number of sub-apertures needed in the AO system is approximately  $(D/r_0)^2$ . The corresponding number of deformable mirror actuators required depends on what geometry is chosen, but it can be approximated by  $(D/r_0)^2$ . Hence the smaller the coherence length  $r_0$  (i.e. the stronger the turbulence is), the more subapertures will be needed.

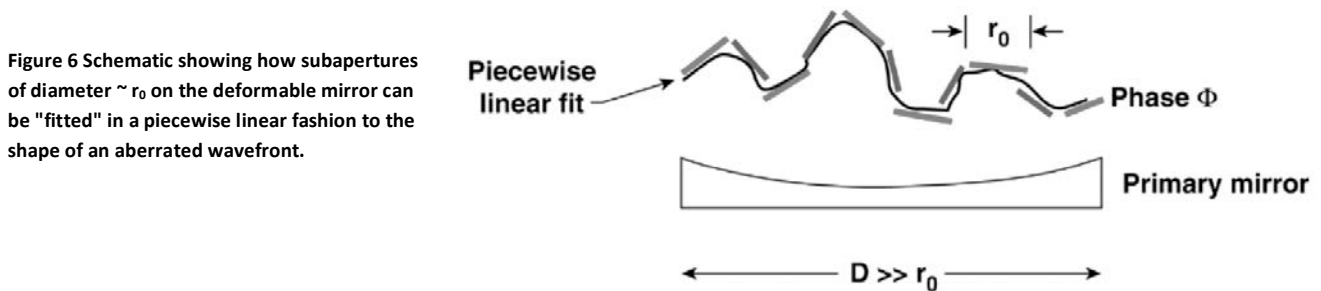


Figure 6 Schematic showing how subapertures of diameter  $\sim r_0$  on the deformable mirror can be "fitted" in a piecewise linear fashion to the shape of an aberrated wavefront.

Some concrete examples may help to develop intuition. Table 1 shows the value of  $D/r_0$  for a variety of telescope diameters and observing wavelengths, assuming that  $r_0(\lambda = 0.5\mu m) = 10\text{ cm}$ . First consider mid-infrared observing wavelengths,  $\lambda = 10\mu m$ . Only for the next generation of extremely large telescopes (e.g. the currently planned E-ELT, GMT, and TMT with diameters 20 - 40 m) is high-order adaptive optics needed for mid-infrared observations, since  $D/r_0 < 3$  for telescope diameters  $\leq 10\text{ m}$ . Next, consider the near-infrared,  $\lambda = 2.2\mu m$ . First-generation adaptive optics systems built for 8-10 m telescopes between 1999 and 2007 (e.g. Gemini North, Christou et al. 2010; Keck, van Dam et al. 2004; Subaru, Minowa et al. 2010) were designed to function at near-infrared wavelengths,  $1.2\mu m \leq \lambda \leq 2.4\mu m$ . One can see from Table 1 that at  $\lambda = 2.2\mu m$ ,  $D/r_0$  is 18.9, so that  $(D/r_0)^2 \approx 360$ . In practice these first-generation AO systems on 8-10 m telescopes had a few hundred

active actuators: for example the Keck AO systems have 240 actuators within the hexagonal pupil; ALTAIR on Gemini North has 177. These systems take advantage of the fact that typical values of  $r_0$  at the Mauna Kea observatories (Dekany 2007) are close to 15 cm rather than 10 cm, and the first-generation systems were not optimized for performance in less-than-median seeing conditions. Finally, we note that AO systems operating at observing wavelengths of  $0.5 - 0.8 \mu\text{m}$  on 8-10 m telescopes will require deformable mirrors with many thousands of actuators, as will AO systems operating in the near-infrared on 30 m class telescopes.

Table 1:  $D/r_0$  for observing wavelengths ranging from  $\lambda = 10 \mu\text{m}$  to  $0.5 \mu\text{m}$ , and for telescopes of different diameter  $D$ . Here  $r_0$  is the atmospheric coherence length (Equation 4), which is assumed to be equal to 10 cm at  $\lambda = 0.5 \mu\text{m}$ .

Observing wavelength ( $\mu\text{m}$ ) $\Rightarrow$	10	2.2	0.8	0.5
Telescope diam. (m) $\downarrow$				
4	1.1	7.6	22.8	40
10	2.7	18.9	56.9	100
30	8.2	56.8	170.7	300

### C. IMPACT OF $r_0$ ON ADAPTIVE OPTICS SYSTEMS: TEMPORAL RESPONSE

The atmospheric coherence length  $r_0$  also plays a key role in determining how quickly an AO system must update its measurement of the turbulent wavefront and command its deformable mirror. This is because atmospheric turbulence can be viewed as a "frozen flow": the detailed structure of turbulence within each eddy evolves slowly compared to the time it takes the larger-scale wind to advect the turbulent structure across one subaperture of the adaptive optics system. Under these conditions the typical timescale over which the AO system must complete its correction is  $\tau_0 \propto r_0 / V_w$  where  $V_w$  is the large-scale wind speed and  $\tau_0$  is the time interval for optical path differences to deviate by a radian of rms phase. Specifically, this is called "Taylor's Frozen Flow Hypothesis" and is valid when 1) the spatial pattern of a random turbulent field is moving with the average velocity of the large-scale wind, and 2) turbulent eddies do not evolve significantly during the time they are carried across a subaperture by the average wind. The above two conditions are generally met for systems in which turbulent velocities are small compared with the large-scale wind speed.

It is informative to look at the more quantitative expression for  $\tau_0$ :

$$\tau_0 \sim 0.3 \left( \frac{r_0}{\bar{V}} \right) \text{ where } \bar{V} \equiv \left[ \frac{\int dz C_N^2(z) |V(z)|^{5/3}}{\int dz C_N^2(z)} \right]^{3/5} \quad (5)$$

Here one sees that in the determination of the "average" wind speed  $\bar{V}$ , the local wind speed  $V(z)$  at an altitude  $z$  is weighted by the turbulence strength  $C_N^2$  at that altitude. In other words, what matters for determining the characteristic timescale for AO correction is having high velocities at altitudes where the turbulence is strong. Note that the typical correction timescale  $\tau_0$  depends only on the subaperture size  $\sim r_0$ , not on the size of the telescope's primary mirror.

To help the reader develop a feel for the numbers, Table 2 shows estimates of both  $\tau_0$  and  $f_0 = 1/\tau_0$  for three observing wavelengths, assuming that  $r_0(\lambda = 0.5\mu m) = 10\text{ cm}$ . It is important to note that for the type of closed-loop feedback system seen in most adaptive optics designs to date, one must sample the measurements of turbulence at about 10 times the final desired closed-loop bandwidth. Thus for example the sampling frequency needed for AO correction at  $\lambda = 0.5\mu m$  is 2 kHz!

Table 2 Timescales  $\tau_0$  and frequencies  $f_0$  required for an adaptive optics system to complete its correction, assuming that  $r_0(\lambda = 0.5\mu m) = 10\text{ cm}$

Wavelength ( $\mu m$ )	$r_0$	$\tau_0 \approx r_0 / V_w$	$f_0 \equiv 1/\tau_0 \approx V_w / r_0$
0.5	10 cm	5 msec	200 Hz
2.2	53 cm	27 msec	37 Hz
10	3.6 m	180 msec	5.6 Hz

#### D. IMPACT OF $r_0$ ON ADAPTIVE OPTICS SYSTEMS: ISOPLANATIC ANGLE

As suggested by Figure 5, measuring the turbulent wavefront by observing a star that is "close" to the astronomical object of interest (in this case a galaxy) only makes sense if the light from the star and the light from the galaxy pass through approximately the same turbulence. Clearly if the star is too far in angular distance from the galaxy, correcting for the turbulence measured in the direction of the star will not produce good AO correction in the direction of the galaxy. The magnitude of this effect is described by the "isoplanatic angle" - qualitatively, the angle on the sky over which the shape of the wavefront is approximately the same.

The quantitative definition of the isoplanatic angle  $\theta_0$  is the size of the angular offset  $\theta$  from the reference star such that

$$\frac{\text{Strehl}(\theta = \theta_0)}{\text{Strehl}(\theta = 0)} = \frac{1}{e} \quad (6)$$

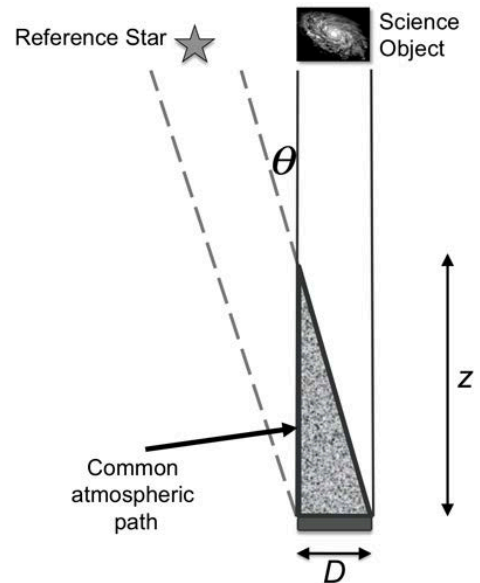
With this definition, the dependence of the isoplanatic angle on the atmospheric turbulence strength  $C_N^2(z)$ , on the wavelength at which the image is being observed  $\lambda = 2\pi/k$ , and on zenith angle  $\zeta$ , is given by

$$\theta_0 = 0.314 (\cos \zeta) \left( \frac{r_0}{\bar{h}} \right) \quad \text{where } \bar{h} \equiv \left( \frac{\int dz z^{5/3} C_N^2(z)}{\int dz C_N^2(z)} \right)^{3/5} \quad (7)$$

A very important point is that the size of the isoplanatic angle is heavily weighted by the turbulence at high altitude  $z$ : what matters within the integral in Equation (7) is the integral over  $z^{5/3} C_N^2(z)$ . The physical reason for this can be seen in Figure 7. The optical paths to the reference star and to the science object overlap less and less as the altitude  $z$  increases. Thus when turbulence is strong at higher altitudes, the common atmospheric path is smaller, and the AO correction of the science object based on measurement in the direction of the reference star will be worse. This

corresponds to a smaller value of the isoplanatic angle  $\theta_0$ .

FIGURE 7 Sensed turbulence seen by the optical path to the reference star and the optical path to the science object, when they are offset in angle by  $\theta$ . The shaded triangular region indicates the volume of turbulence that is common to both optical paths. For turbulence located at higher altitudes  $z$ , the common volume becomes smaller and smaller.



Conversely if almost all of the atmospheric turbulence is located close to the ground, it will fall well within the region that is sensed in common by both optical paths and the corresponding isoplanatic angle  $\theta_0$  will be large. This provides the motivation for "ground-layer AO systems" in which only the low-altitude turbulence is corrected. The result is an imperfectly corrected image, because there is inevitably turbulence located above the ground layer that is not being taken into account. However the effective isoplanatic angle for the correction can be very large.

### III. BIBLIOGRAPHY

- J. Beckers, "Adaptive Optics for Astronomy: Principles, Performance, and Applications," 1993, Ann. Rev. Astron. Astrophys., 31, 13
- J. Christou, et al., 2010, "ALTAIR performance and updates at Gemini North," SPIE Conference Series, Vol. 7736, 62.
- R. Davies and M. Kasper, "Adaptive Optics for Astronomy," Sept. 2012, Ann. Revs. Astro. Astrophys.,
- R. Dekany, 2007, "Mauna Kea Ridge (MKR) Turbulence Models," Keck Adaptive Optics Note 503
- R. Q. Dutton, "The Adaptive Optics Revolution: A History," University of New Mexico Press (Albuquerque, 2009)
- S. Esposito et al., "Large Binocular Telescope Adaptive Optics System: New achievements and perspectives in adaptive optics," 2011, in "Astronomical Adaptive Optics Systems and Applications IV". Edited by Tyson, Robert K.; Hart, Michael. Proc. SPIE, 8149, pp. 814902-814902-10
- D. L. Fried, 1965, "Statistics of a geometrical representation of wavefront distortion," J. Opt. Soc. America, 55, 1427.
- J. W. Hardy, 1998, "Adaptive Optics for Astronomical Telescopes," (Oxford University Press, Oxford).
- J. Kubby, editor, "Adaptive Optics for Biological Imaging," (CRC Press/Taylor & Frances Group, 2012)
- Lincoln Laboratory Journal, Special Issue on Adaptive Optics, Spring 1992, Volume 5, number 1
- Y. Minowa et al., 2010, "Performance of Subaru adaptive optics system AO188," Adaptive Optics Systems II,

edited by Brent L. Ellerbroek, Michael Hart, Norbert Hubin, Peter L. Wizinowich, Proc. SPIE 7736, 77363N

J. Porter, H. Queener, J. Lin, K. Thorne, & A. Awwal, editors; "Adaptive Optics for Vision Science," (Wiley, NY, 2006)

F. Roddier, "Adaptive Optics in Astronomy," Cambridge University Press (Cambridge, 1999)

M. C. Roggeman, B. M. Welsh, & R. Q. Fugate, "Improving the resolution of ground-based telescopes," 1997, Rev. Mod. Phys., 69, 437

V. I. Tatarski, 1961, "Wave Propagation in a Turbulent Medium," (McGraw-Hill, New York).

R. K. Tyson, "Principles of Adaptive Optics, Third Edition," Academic Press (Boston, 2012)

M. A. van Dam et al., 2004, "Performance of the Keck Observatory adaptive-optics system," Applied Optics 43, 5458.